Pergamon

Engineering Fracture Mechanics Vol. 60, No. 2, pp. 205–219, 1998

Printed in Great Britain
PII: S0013-7944(97)00099-4
0013-7944/98 $19.00 + 0.00

PLANE-STRESS ASYMPTOTIC FIELDS FOR INTERFACE CRACK BETWEEN ELASTIC AND PRESSURE-SENSITIVE DILATANT MATERIALS

HONGRONG YU†, YONG-LI WU and GUOCHEN LI

Institute of Mechanics, Chinese Academy of Sciences, Beijing 100080, People's Republic of China

Abstract—In this paper, the plane-stress interface crack-tip fields between pressure-sensitive dilatant material and linear elastic material are investigated. Applying the stress–strain relation for the pressure-sensitive dilatant material, we have obtained an exact asymptotic solution of plane-stress tip fields for two types of cracks, one of which is along the interface and another is perpendicular to the interface between the linear elastic material and pressure-sensitive dilatant material. The obtained fields satisfy the condition of the continuity of tractions at the interface and the traction-free conditions on the crack faces. For the first type of crack, the eigenvalue s is irrelevant to the pressure sensitivity parameter μ and is equal to $-1/(n+1)$, which is the eigenvalue of the HRR fields for homogeneous media without pressure sensitivity. While in the second type of crack, both s and μ increase simultaneously when n is fixed, but s tends to zero if μ is approaching to $\mu_{\lim}$.

Keywords—asymptotic field, interface crack, pressure-sensitive, dilatant material.

1. INTRODUCTION

RECENTLY, THE researches on the mechanical behavior of some materials that exhibit pressure-sensitive dilatancy have attracted much attention, because these materials cannot be described by the classical plasticity theories which neglect the effect of hydrostatic pressure. The examples of these materials may include toughened structural polymers and ceramics. The results reported by Spitzig and Richmond [1], Carapellucci and Yee [2], Sue and Yee [3] and Chen and Morel [4] have confirmed that pressure-sensitive yielding has a strong effect on the plastic deformation and fracture behavior of the materials studied.

With regards to engineering materials, many researches have focused their attention on the interfaces because defects may occur easily in the interfacial regions and cause damage to the materials. Williams [5] was the first who analyzed a two-dimensional elastic problem of a crack lying along the interface between two dissimilar isotropic media by using eigenfunction method. Later, Cheepanov [6], Erdogan [7], Rice and Sih [8, 9] and Malyshev and Salganik [10] presented the similar problem by utilizing different methods. Recently Hutchinson *et al.* [11], Rice [12], Shih and Asaro [13] and Zywicz and Parks [14] have summarized and developed those early research results.

Shih and Asaro [13, 15, 16] originally investigated the solutions for an interface crack in elastic–plastic materials. A solution for the elastic–perfectly plastic, small-scale yielding interfacial crack-tip fields in bimaterials has been reported by Zywicz and Parks [17]. Wang [18] presented an exact asymptotic field analysis for a crack which lies along the interface of an elastic–plastic medium and a linear elastic medium. The problem of a plane strain crack lying along an interface between a rigid substrate and elastic–plastic dilatant medium has been studied by Yuan [19].

In this paper, we studied the plane-stress interface crack-tip fields between pressure-sensitive dilatant material and linear elastic material. Based on a simple pressure-sensitive yield criterion introduced by Drucker and Prager [20] and modified by Li and Pan [21], we obtain an exact asymptotic solution of plane-stress tip field for two types of cracks, one of which is along the interface between a linear elastic material and pressure-sensitive dilatant material and another is perpendicular to the interface.

†Author to whom all correspondence should be addressed.

2. BASIC EQUATIONS

Figure 1 shows an interfacial crack between medium 2 that is a linear elastic material in the lower half plane and medium 1 that is a pressure-sensitive dilatant material in the upper half plane.

For the sake of simplicity, it is assumed that both materials have the same elastic modulus and Poisson's ratio, i.e. $E_1 = E_2 = E$, $\nu_1 = \nu_2 = \nu$.

For the plane stress, the stress–strain relations for the elastic material 2 can be expressed as

$$\varepsilon_{ij} = \frac{1+\nu}{E} S_{ij} + \frac{1-2\nu}{3E} \sigma_{kk} \delta_{ij}. \tag{1}$$

The simple pressure-sensitive yielding criterion given by Li and Pan[21] can be adopted for material 1 as

$$\tau_{ge} = \tau_e + \mu\sigma_m = \psi(\sigma_{ij}) \tag{2a}$$

$$\tau_e = (S_{ij}S_{ij}/2)^{1/2},\ S_{ij} = \sigma_{ij} - \sigma_m\delta_{ij},\ \sigma_m = \sigma_{kk}/3 \tag{2b}$$

where $\psi(\sigma_{ij})$ represents the yield surface in stress space, τ_{ge} is generalized effective shear stress, μ is a pressure sensitive factor. When $\mu = 0$, it means that the effect of hydrostatic pressure is neglected.

In this analysis, it is assumed that the elastic–plastic behavior for material 1 in shear can be expressed as

$$\frac{\gamma}{\gamma_0} = \frac{\tau}{\tau_0} + \alpha\left(\frac{\tau}{\tau_0}\right)^n \tag{3}$$

where τ and γ are, respectively, the shear stress and shear strain, τ_0 and γ_0 are the reference shear stress and reference strain, n is the strain hardening exponent, α is a material constant.

In the asymptotic analysis for near-crack-tip field, the elastic strains are much smaller in comparison with the plastic strains and, therefore, can be neglected. In this sense, we have the constitutive equation

$$\frac{\varepsilon_{ij}^{p}}{\gamma_0} = \alpha\left(\frac{t_{ge}}{\gamma_0}\right)^n\left(\frac{S_{ij}}{2\tau_e} + \frac{\mu}{3}\delta_{ij}\right). \tag{4}$$

For the case of plane stress we have

$$\sigma_{zz} = 0. \tag{5}$$

Now the general form of strain–stress relations given in eq. (4) can be specified, in polar coordinates, by stating

$$\frac{\varepsilon_{rr}}{\gamma_0} = \frac{1}{3}\alpha\left(\frac{\tau_{ge}}{\tau_0}\right)^n\left(\frac{\sigma_{rr} - \sigma_{\theta\theta}}{2\tau_e} + \mu\right) \tag{6a}$$

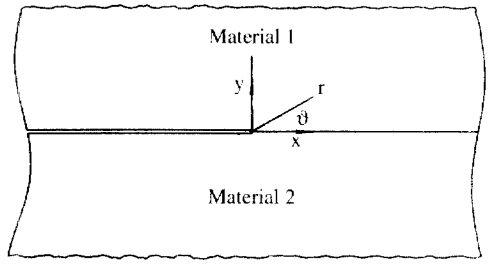

Fig. 1. An interfacial crack I between a linear elastic material and a pressure-sensitive dilatant material.

$$\frac{\varepsilon_{\theta\theta}}{\gamma_0} = \frac{1}{3}\alpha\left(\frac{\tau_{ge}}{\tau_0}\right)^n\left(\frac{\sigma_{\theta\theta} - \sigma_{rr}}{2\tau_e} + \mu\right) \tag{6b}$$

$$\frac{\varepsilon_{r\theta}}{\gamma_0} = \frac{1}{2}\alpha\left(\frac{\tau_{ge}}{\tau_0}\right)^n\frac{\sigma_{r\theta}}{\tau_e} \tag{6c}$$

$$\varepsilon_{zz} = \frac{1}{3}\alpha\left(\frac{\tau_{ge}}{\tau_0}\right)^n\left(-\frac{\sigma_{rr} + \sigma_{\theta\theta}}{2\tau_e} + \mu\right) \tag{6d}$$

where

$$\tau_e = \frac{\sigma_e}{\sqrt{3}} = \frac{1}{\sqrt{3}}(\sigma_{rr}^2 + \sigma_{\theta\theta}^2 - \sigma_{rr}\sigma_{\theta\theta} + 3\sigma_{r\theta}^2)^{1/2}$$

$$\tau_{ge} = \frac{\sigma_{ge}}{\sqrt{3}} = \frac{1}{\sqrt{3}}(\sigma_{rr}^2 + \sigma_{\theta\theta}^2 - \sigma_{rr}\sigma_{\theta\theta} + 3\sigma_{r\theta}^2)^{1/2} + \frac{\mu}{3}(\sigma_{rr} + \sigma_{\theta\theta}).$$

The stress components in polar coordinate are expressed by stress function $\varphi(r, \theta)$ as

$$\sigma_{rr} = \frac{1}{r}\frac{\partial\varphi}{\partial r} + \frac{1}{r^2}\frac{\partial^2\varphi}{\partial\theta^2} \quad \sigma_{\theta\theta} = \frac{\partial^2\varphi}{\partial r^2} \quad \sigma_{r\theta} = -\frac{\partial}{\partial r}\left(\frac{1}{r}\frac{\partial\varphi}{\partial\theta}\right). \tag{7}$$

Then the equations of equilibrium can be automatically satisfied.

The relations of displacement–strain are

$$\varepsilon_{rr}\frac{\partial u_r}{\partial r} \quad \varepsilon_{\theta\theta} = \frac{1}{r}\frac{\partial u_\theta}{\partial\theta} + \frac{u_r}{r} \quad \varepsilon_{r\theta} = \frac{1}{2}\left(\frac{1}{r}\frac{\partial u_r}{\partial\theta} + \frac{\partial u_\theta}{\partial r} - \frac{u_\theta}{r}\right). \tag{8}$$

The strain compatibility equation is

$$\frac{1}{r}\frac{\partial^2(r\varepsilon_{\theta\theta})}{\partial r^2} + \frac{1}{r^2}\frac{\partial^2\varepsilon_{rr}}{\partial\theta^2} - \frac{1}{r}\frac{\partial\varepsilon_{rr}}{\partial r} - \frac{2}{r^2}\frac{\partial^2(r\varepsilon_{r\theta})}{\partial r\partial\theta} = 0. \tag{9}$$

In order to ensure the tractions to be continuous on the interface, we assume that the stress field in the whole tip zone has the same singularity for both materials. Let

$$\varphi(r\text{-}\theta) = Kr^{s+2}F(\theta). \tag{10}$$

Substituting eq. (10) into eq. (7), we can obtain

$$\sigma_{ij} = Kr^s\tilde{\sigma}_{ij}(\theta) \tag{11}$$

$$\tilde{\sigma}_{rr}(\theta) = F'' + (2 + s)F \tag{12a}$$

$$\tilde{\sigma}_{\theta\theta}(\theta) = (2 + s)(1 + s)F \tag{12b}$$

$$\tilde{\sigma}_{r\theta} = -(1 + s)F'. \tag{12c}$$

The corresponding strains are then

$$\varepsilon_{ij} = \tilde{\alpha}\tilde{K}^n r^{ns}\tilde{\varepsilon}_{ij} \tag{13}$$

$$\tilde{\varepsilon}_{rr} = \frac{1}{3}\tilde{\tau}_{ge}^n\left(\frac{2\tilde{\sigma}_{rr} - \tilde{\sigma}_{\theta\theta}}{2\tilde{\tau}_e} + \mu\right) \tag{14a}$$

$$\tilde{\varepsilon}_{\theta\theta} = \frac{1}{3}\tilde{\tau}_{ge}^n\left(\frac{2\tilde{\sigma}_{\theta\theta} - \tilde{\sigma}_{rr}}{2\tilde{\tau}_e} + \mu\right) \tag{14b}$$

$$\tilde{\varepsilon}_{r\theta} = \frac{1}{2}\tilde{\tau}_{\mathrm{ge}}^{n}\frac{\tilde{\sigma}_{r\theta}}{\tilde{\tau}_{\mathrm{e}}} \tag{14c}$$

$$\tilde{\varepsilon}_{zz} = \frac{1}{3}(\tilde{\tau}_{\mathrm{ge}})^{n}\left(-\frac{\tilde{\sigma}_{rr}+\tilde{\sigma}_{\theta\theta}}{2\tilde{\tau}_{\mathrm{ge}}}+\mu\right) \tag{14d}$$

where

$$\tilde{\tau}_{\mathrm{e}} = \frac{\tilde{\sigma}_{\mathrm{e}}}{\sqrt{3}} = \frac{1}{\sqrt{3}}(\tilde{\sigma}_{rr}^{2}+\tilde{\sigma}_{\theta\theta}^{2}-\tilde{\sigma}_{rr}\tilde{\sigma}_{\theta\theta}+3\tilde{\sigma}_{r\theta}^{2})^{1/2}$$

$$\tilde{\tau}_{\mathrm{ge}} = \frac{\tilde{\sigma}_{\mathrm{ge}}}{\sqrt{3}} = \frac{1}{\sqrt{3}}(\tilde{\sigma}_{rr}^{2}+\tilde{\sigma}_{\theta\theta}^{2}-\tilde{\sigma}_{rr}\tilde{\sigma}_{\theta\theta}+3\tilde{\sigma}_{r\theta}^{2})^{1/2}+\frac{\mu}{3}(\tilde{\sigma}_{rr}+\tilde{\sigma}_{\theta\theta}).$$

The strain compatibility eq. (9) can be represented as

$$\left(\frac{\mathrm{d}^{2}}{\mathrm{d}\theta^{2}}-ns\right)\left[\tilde{\tau}_{\mathrm{ge}}^{n}\left(\frac{2F''+(2+s)(-s)F}{2\tilde{\tau}_{\mathrm{e}}}\right)+\mu\right]+3(ns+1)(s+1)\frac{\mathrm{d}}{\mathrm{d}\theta}\left(\tilde{\tau}_{\mathrm{ge}}^{n}\frac{F'}{\tilde{\tau}_{\mathrm{e}}}\right)$$

$$+ns(ns+1)\tilde{\tau}_{\mathrm{ge}}^{n}\left[\frac{(2+s)(1+2s)F-F''}{2\tilde{\tau}_{\mathrm{e}}}+\mu\right]=0. \tag{15}$$

For the linear elastic material 2, we have the equation

$$F''''+[(s+2)^{2}+s^{2}]F''+s^{2}(s+2)^{2}F=0. \tag{16}$$

The general solution for this equation is

$$F = B_{1}\cos(s\theta)+B_{2}\sin(s\theta)+B_{3}\cos(s+2)\theta+B_{4}\sin(s+2)\theta. \tag{17}$$

The traction-free conditions on the crack faces require

$$\sigma_{\theta\theta}|_{\theta=\pm\pi} = \sigma_{r\theta}|_{\theta=\pm\pi} = 0 \tag{18}$$

which means

$$F(\pi) = F'(\pi) = F(-\pi) = F'(-\pi) = 0. \tag{19}$$

The continuity of tractions on the interface requires the following:

$$\tilde{\sigma}_{\theta\theta}(0^{+}) = \tilde{\sigma}_{\theta\theta}(0^{-})\ \tilde{\sigma}_{r\theta}(0^{+}) = \tilde{\sigma}_{r\theta}(0^{-}). \tag{20}$$

From eq. (20) we obtain

$$F(0^{+}) = F(0^{-})\ F'(0^{+}) = F'(0^{-}). \tag{21}$$

Ignoring the rigid displacements, we obtain from eq. (8) the displacements in material 1:

$$u_{\beta} = \tilde{\alpha}\tilde{K}r^{(1+ns)}\tilde{u}_{\beta}(\theta) \tag{22}$$

$$\tilde{u}_{r} = \tilde{\varepsilon}_{rr}/(1+ns)\ \tilde{u}_{\theta} = (2\tilde{\varepsilon}_{r\theta}-\tilde{u}_{r}{}')/ns. \tag{23}$$

As pointed out by Shih and Asaro[13] for a bimaterial, the material with a lower hardening capacity responds at the interface as if it is bonded to a rigid substance, and so we have

$$\tilde{u}_{r} = \tilde{u}_{\theta} = 0 \text{ at } \theta = 0^{+} \tag{24}$$

which can be written in term of the stresses as

$$2\tilde{\sigma}_{rr} - \tilde{\sigma}_{\theta\theta} + 2\mu\tilde{\tau}_e 0$$

$$2\tilde{\sigma}_{rr}' - \tilde{\sigma}_{\theta\theta}' + 2\mu\tilde{\tau}_e' - 6(ns+1)\tilde{\sigma}_{r\theta} = 0 \text{ at } \theta = 0^+. \tag{25}$$

3. SOLUTIONS OF ASYMPTOTIC FIELDS

Combining the nonlinear eq. (15) and the boundary conditions of eqs (19) and (25), the eigenvalue s and eigenfunction F within the region of $0 \leq \theta \leq \pi$ can be found for the pressure-sensitive material 1 by using the shooting method. The initial value of $F(0^+)$ is taken as unity for easy handling. After s reaches $-1/(1+n)$ and a value of $F'(0^+)$ is given, $F''(0^+)$ and $F'''(0^+)$ can be obtained from eq. (25), by using the fourth-order Runge–Kutta method with automatic step-size control. Equation (15) can be integrated from $\theta = 0^+$ to $\theta = \pi$. The results at $\theta = \pi$ generally cannot fully satisfy the boundary conditions. Subsequently adjust s and the initial

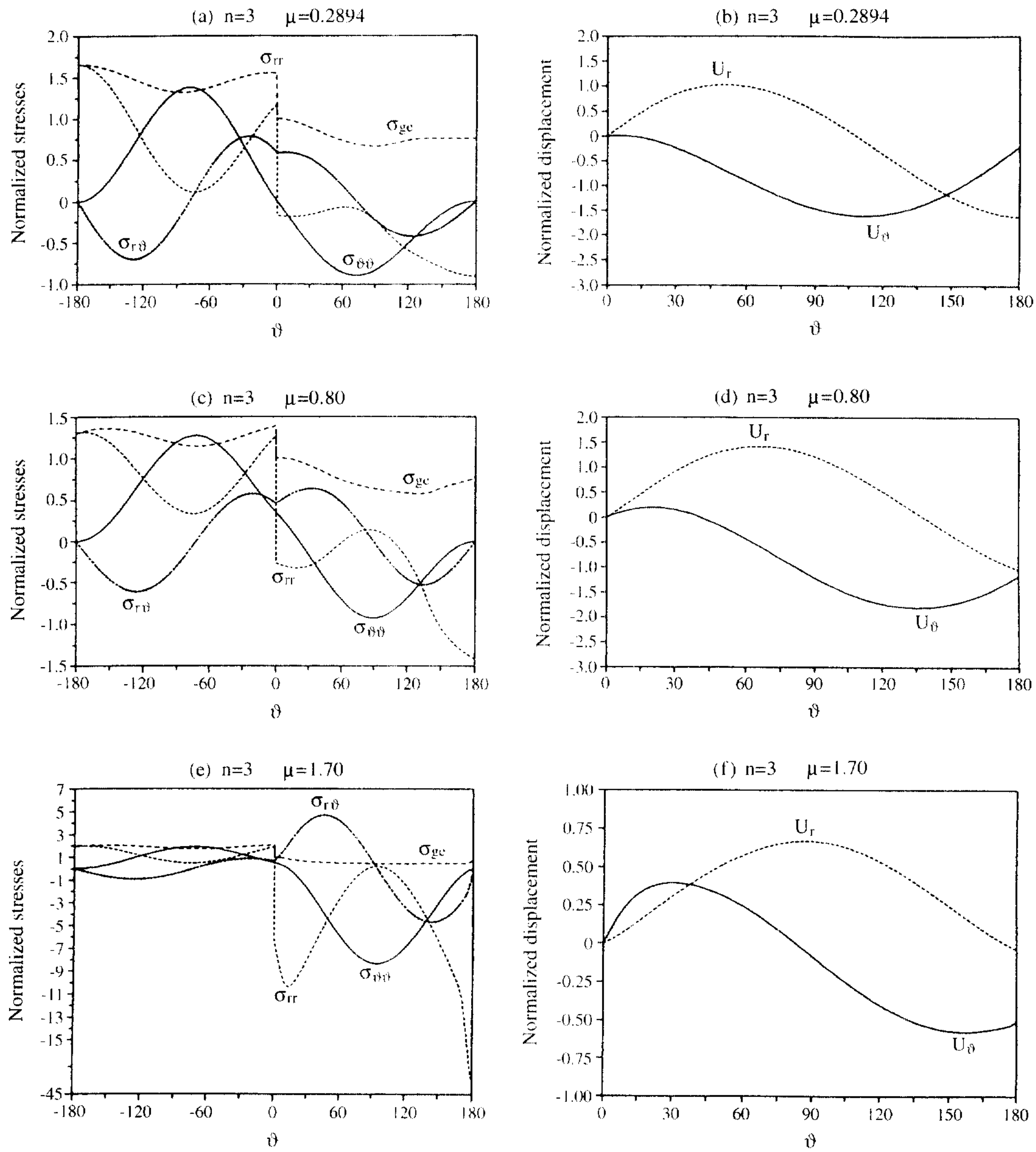

Fig. 2. θ-variation of the stresses $\tilde{\sigma}_{ij}$ in the whole region and the displacements $\tilde{u}_i$ in the plastic region near the tip of interface crack 1 ($n = 3$).

value $F'(0^+)$ by step and repeat the process until the conditions of eq. (19) are satisfied within the limited error.

After the $F(0^+)$ and $F'(0^+)$ used for the pressure-sensitive material are obtained, the coefficients B_1, B_2, B_3 and B_4 given in eq. (17) for the elastic region can be determined by employing eqs (19) and (21).

In order to ensure the existence of solution, when dealing with all the values chosen for the strain hardening exponent n, μ must satisfy the following inequality relation:

$$1 - \mu^2/3 > 0 \tag{26}$$

which means

$$\mu < \mu_{\mathrm{lim}}, \ \mu_{\mathrm{lim}} = \sqrt{3}.$$

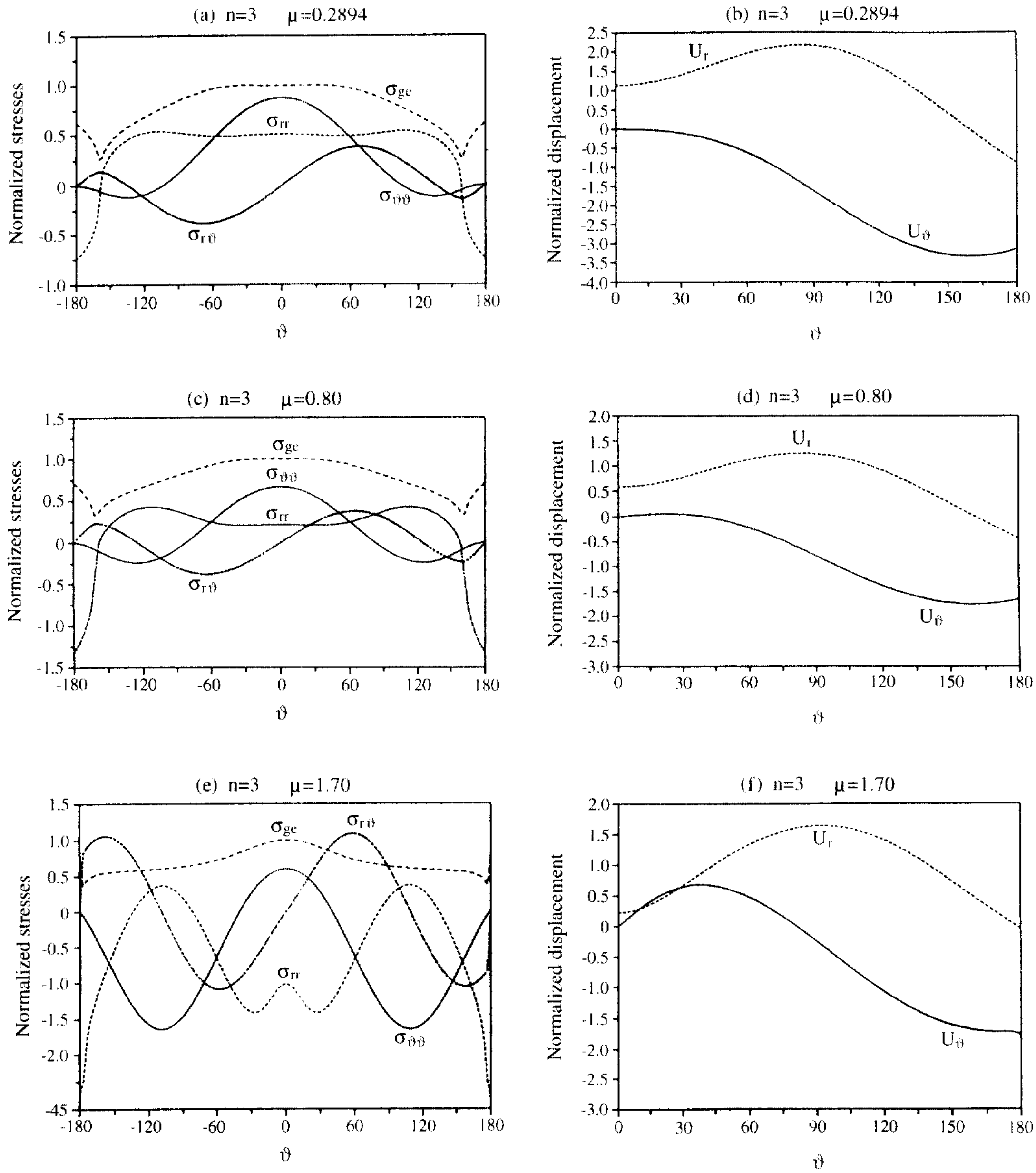

Fig. 3. θ-variation of the stresses $\tilde{\sigma}_{ij}$ in the whole region and the displacements $\tilde{u}_i$ in the upper region near the crack tip in homogenous material ($n = 3$).

A mixed parameter M^p is defined as that proposed by Shih[22], i.e.

$$M^{p} = \frac{2}{\pi} tg^{-1}\left[\frac{\tilde{\sigma}_{\theta\theta}(0)}{\tilde{\tau}_{r\theta}(0)}\right].$$

It is easy to see that $M^p = 1$ for mode I while $M^p = 0$ for mode II.

Figures 2–7 show the θ-variations of the stresses $\tilde{\sigma}_{ij}(\theta)$ and the displacements $\tilde{u}_i$. For comparison sake, we give the results for the case of bimaterial and also the case of the homogenous pressure-sensitive material both subjected to mode I loading. All the stresses are normalized by taking the $((\tilde{\sigma}_{ge}))_{max}$ of plastic region equal to unity. Figures 2 and 3 demonstrate the results of typical high-hardening material when $n = 3$ associated with $\mu = 0.2894$, 0.8 and 1.7. Table 1 lists the value of M^p for the bimaterials. We cannot find any solution that is based on the HRR-type formulation for $\mu < 0.2894$. Figures 4 and 5 and Table 2 give the

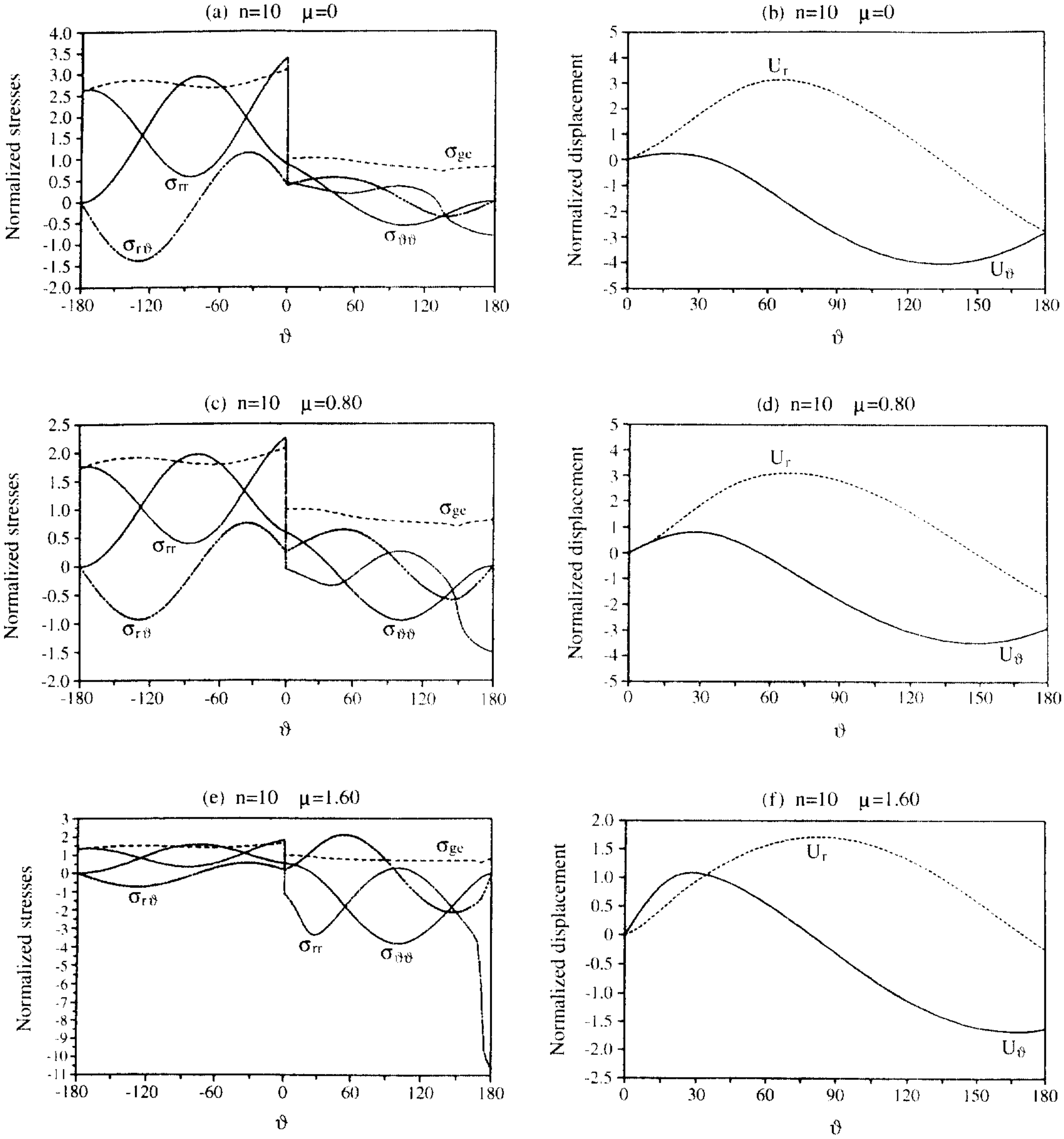

Fig. 4. θ-variation of the stresses $\tilde{\sigma}_{ij}$ in the whole region and the displacements $\tilde{u}_i$ in the plastic region near the tip of interface crack I ($n = 10$).

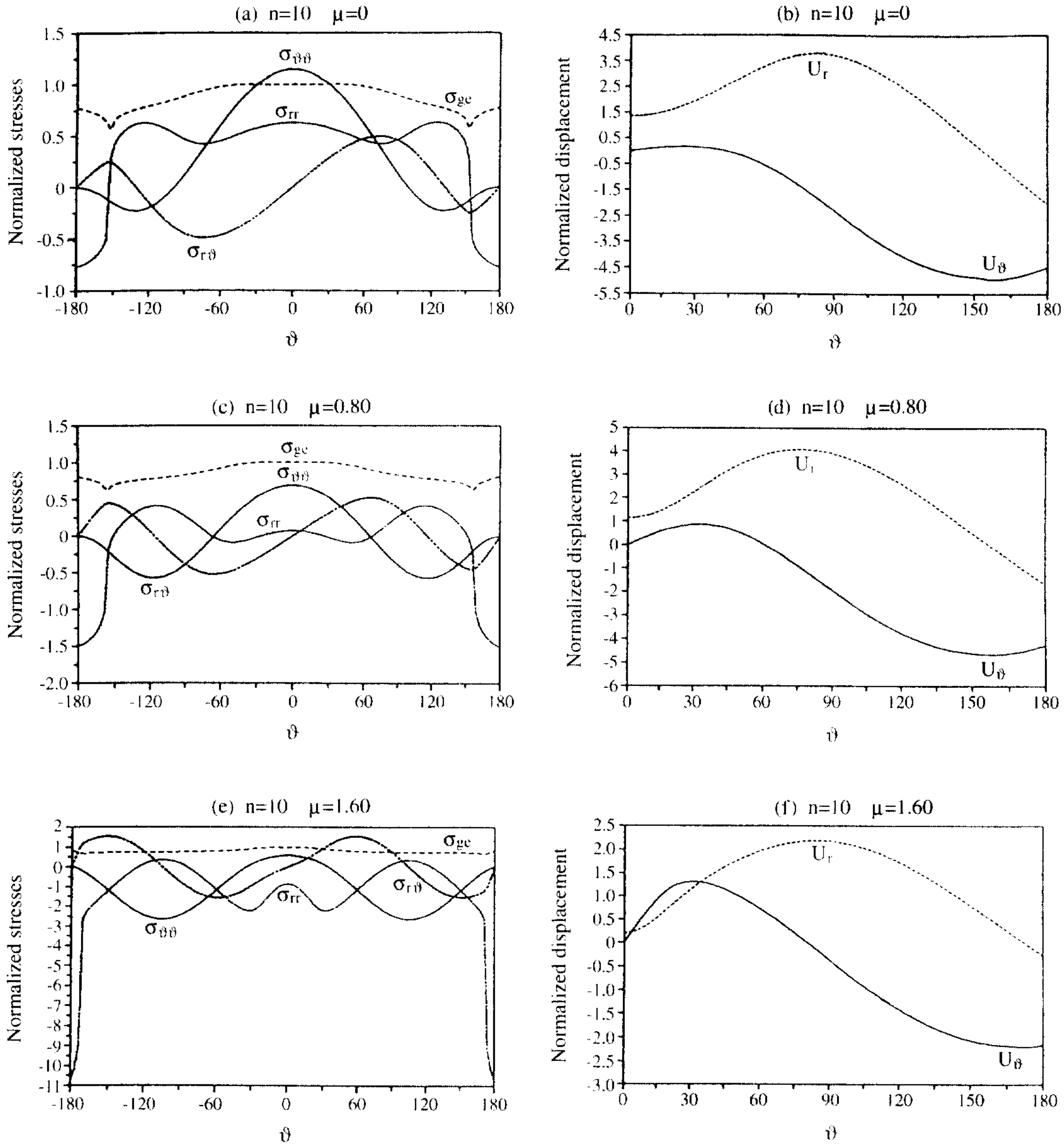

Fig. 5. θ-variation of the stresses $\tilde{\sigma}_{ij}$ in the whole region and the displacements $\tilde{u}_i$ in the upper region near the crack tip in the homogenous material ($n = 10$).

results of the typical low-hardening material of $n = 10$ for $\mu = 0.0$, 0.8 and 1.6. In order to take a better view of the problem, the results of very low-hardening materials of $n = 20$ are also shown in Figs 6 and 7 and Table 3. In all cases, it is found that s can be evaluated as $-1/(n+1)$, which is equal to the eigenvalue of the HRR fields for homogenous media which have no pressure sensitivity.

3.1. *Comparison between the solutions of the bimaterial and the homogenous material*

From the Figs 2, 4 and 6 illustrated for bimaterials, we can see that the radial stress $\tilde{\sigma}_{rr}$ has a radical change at the two sides of the interface. The stress $\tilde{\sigma}_{rr}$ in the region of $-\pi \le \theta \le 0$ is always positive. The situation changes in the cases of Figs 3, 5 and 7 shown for the homogenous material. The shear stress $\tilde{\sigma}_{r\theta}$ of the bimaterial is positive in the elastic region nearby the interface, but negative when approaching the crack face. The shear stress $\tilde{\sigma}_{r\theta}$ of the homogenous material has antisymmetric distribution in the two regions. The circumferential stress $\tilde{\sigma}_{\theta\theta}$ of homogenous material has a peak value at $\theta = 0$ and two valleys nearby $\theta = \pm 120°$. However,

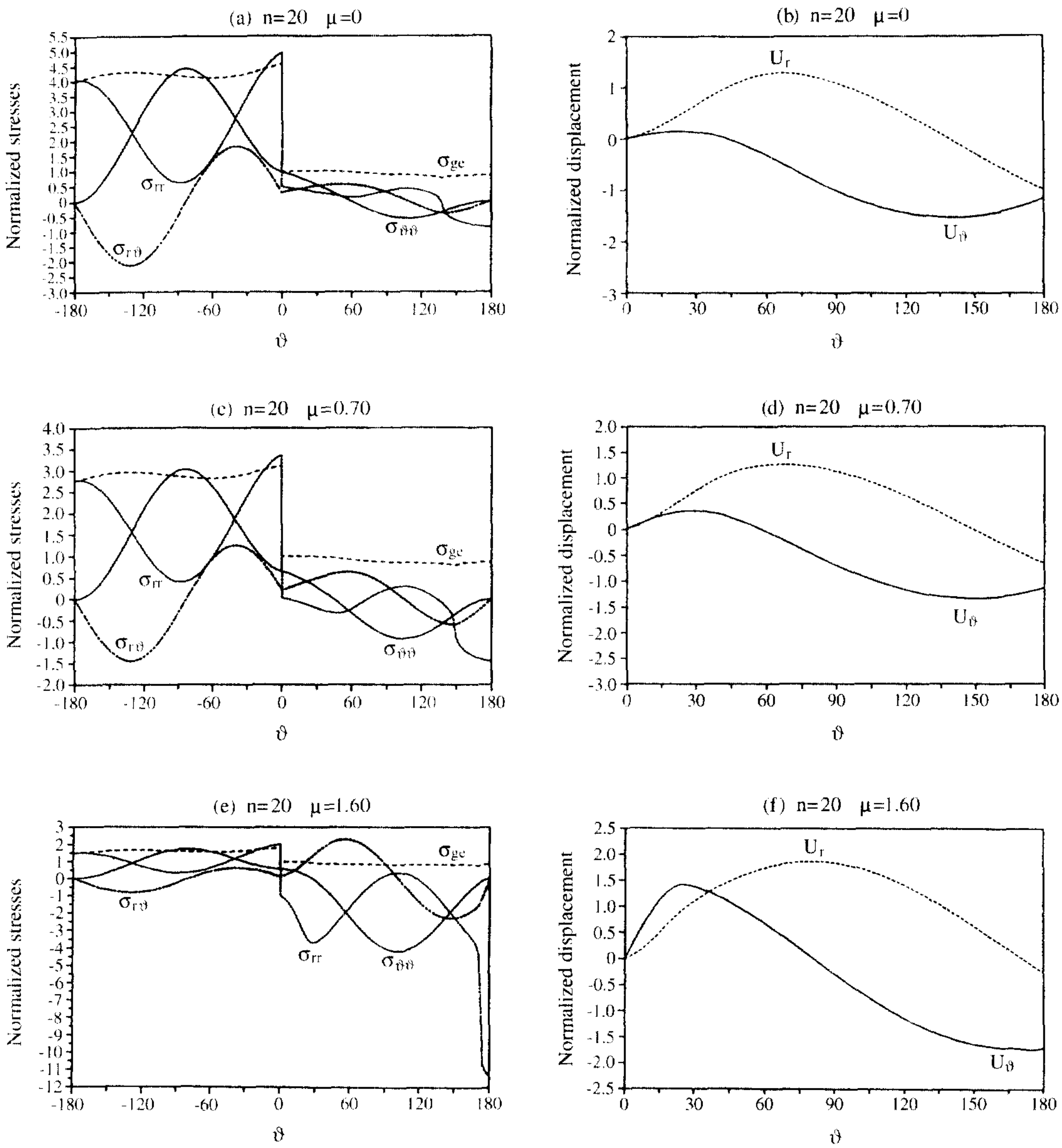

Fig. 6. θ-variation of the stresses $\tilde{\sigma}_{ij}$ in the whole region and the displacements $\tilde{u}_i$ in the plastic region near the tip of interface crack I (n = 20).

for the bimaterial it has one peak (tension) in the elastic region of the material 2 and one valley (compression) in the material 1.

3.2. *The effect of varying μ on the asymptotic fields*

It can be obviously seen from Figs 2–7 that the pressure-sensitive dilatant parameter μ has a strong effect on the distribution of the stresses along circumferential direction θ.

We can also see from Figs 2, 4 and 6 that within the region of $0^\circ \leq \theta \leq 120^\circ$ there exists a maximum value of the radial stress $\tilde{\sigma}_{rr}$. When n is fixed, μ has only a weak effect on the value of $(\tilde{\sigma}_{rr})_{\max}$. When n = 10 and 20, the stress $\tilde{\sigma}_{rr}$ varies sharply near a certain angle θ_0 in the region of the pressure-sensitive material. This angle of θ_0 gradually approaches to π as μ increases. If n = 3, the radial stress $\tilde{\sigma}_{rr}$ near the crack face drops steeply when μ is close to $\mu_{\lim}$. It can also be seen that the largest value of $\tilde{\sigma}_{\theta\theta}$ in compression increases while its smallest value in tension decreases or changes slightly as μ increases. For the shear stress $\tilde{\sigma}_{r\theta}$, its maximum value decreases and its minimum value increases within the region $0 \leq \theta \leq \pi$ as μ increases. However, the general trend changes inversely within the region $-\pi \leq \theta \leq 0$.

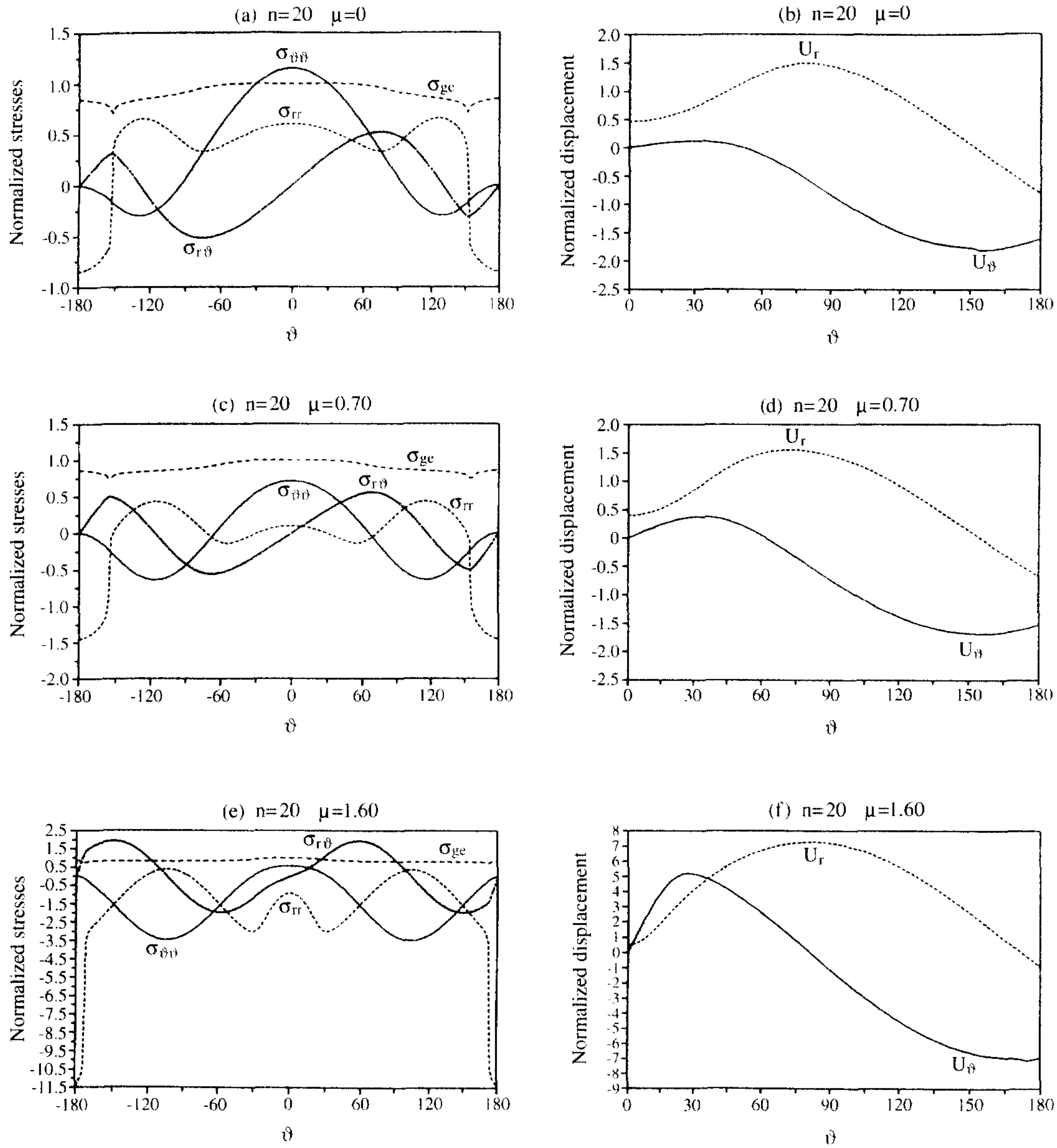

Fig. 7. θ-variation of the stresses $\tilde{\sigma}_{ij}$ in the whole region and the displacements $\tilde{u}_i$ in the upper region near crack tip in homogeneous material ($n = 20$).

3.3. *Mixities of crack-tip fields*

The numerical results given in Tables 1–3 show that the mixities do not approach 1 even for a low-hardening material where $n = 20$, since the stress fields near the crack tip are generally mixed by $\sigma_{\theta\theta}$ and $\sigma_{r\theta}$ as can be seen from Figs 2, 4 and 6. This characteristic behavior of the plane-stress condition is quite different from that of the corresponding plane-strain results reported by Yuan [19]. The leading-order fields of the opening crack model are dominated by the mode I stress in Yuan's report and only his second-order solutions contain substantial mode II components, but the mode-mixity of the second-order fields is strongly affected by the

Table 1. The mixities of crack I ($n = 3$)

μ	M^{p}
0.2894	0.00137909
0.80	0.41895918
1.70	0.40999660

Table 2. The mixities of crack I ($n = 10$)

μ	M^p
0.00	0.74425483
0.80	0.74992528
1.60	0.79380369

Table 3. The mixities of crack I ($n = 20$)

μ	M^p
0.00	0.81074398
0.70	0.82389305
1.60	0.88102336

pressure sensitivity. The asymptotic plane-strain solutions for an interface crack between a rigid substrate and an elastoplastic power-law medium under J_2 deformation theory have been given by Wang[18]. His numerical results have the same trend as that of Yuan and the solutions are near to mode I for both $n = 3$ and 10. The different features can be explained by the diminishing of the transversal stress components (σ_{zz}, σ_{zr}, $\sigma_{z\theta}$) and the relaxing of triaxial stress restraint under the plane-stress condition. Then, in order to satisfy the restriction condition of eq. (24) for displacements at the interface, the shearing stress $\sigma_{r\theta}$ must participate and play an important role. This shearing reaction becomes tenuous when strain hardening effect lowers to $n = 20$, as seen in Table 3.

4. SOLUTION FOR CRACK PERPENDICULAR TO INTERFACE

Figure 8 shows another type of crack called crack II. This crack lies only in material 1 and its tip touches perpendicularly the interface between materials 1 and 2. The external load is also taken to be remote uniform tension. Because of the symmetry of geometry and loading we can write for the material 2 the following equation:

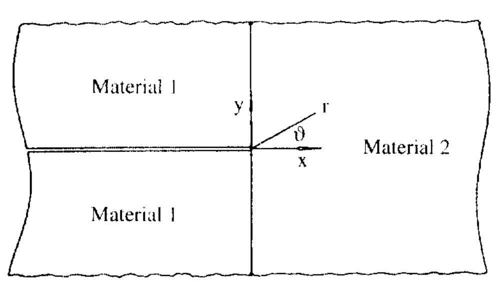

Fig. 8. The crack II that lies in medium 1 with its tip perpendicularly touching the interface of a linear elastic material and a pressure-sensitive dilatant material.

Table 4. The values s varying with respect to μ and n for the case of crack II

	$n = 2$	$n = 3$	$n = 6$	$n = 10$	$n = 20$	$n = 100$
$\mu = 0.00$	−0.21053223	−0.16391430	−0.10260719	−0.07027791	−0.04027163	−0.00945560
$\mu = 0.20$	−0.18201820	−0.14220083	−0.09017938	−0.06270429	−0.03684977	−0.00914212
$\mu = 0.40$	−0.14819661	−0.11604172	−0.07447176	−0.05257957	−0.03179594	−0.00853145
$\mu = 0.60$	−0.10498205	−0.08220359	−0.05326322	−0.03818212	−0.02384565	−0.00716635
$\mu = 0.80$	−0.03864432	−0.02998909	−0.01948567	−0.01417060	−0.00920895	−0.00330598
$\mu = \mu_{lim}$	−0.00000260	−0.00000199	−0.00000128	−0.00000114	−0.00000076	−0.00000025

$$F = B_1 \cos(s\theta) + B_3 \cos(s+2)\theta. \tag{27}$$

We have the restrictions on displacements along the interface

$$U_r = U_\theta = 0 \text{ at } \theta = (\pi/2)^+. \tag{28}$$

This conditions can be expressed in terms of stresses; then they become

$$2\tilde{\sigma}_{rr} - \tilde{\sigma}_{\theta\theta} + 2\mu\tilde{\tau}_e = 0$$

$$2\tilde{\sigma}_{rr}{}' - \tilde{\sigma}_{\theta\theta}{}' + 2\mu\tilde{\tau}_e{}' - 6(ns+1)\tilde{\sigma}_{r\theta} = 0 \text{ at } \theta = (\pi/2)^+. \tag{29}$$

Using the same method as stated above we obtain the solution for this case. The eigenvalue s for various n and μ are listed in Table 4. The numerical results show that the eigenvalue s is not equal to $-1/(n+1)$, but increases as μ increases under fixed value of n. $\mu_{\rm lim}$ is irrelevant to n and is equal to 0.86614. The eigenvalue s is vanishing at $\mu_{\rm lim}$. When $\mu > \mu_{\rm lim}$, the displacement

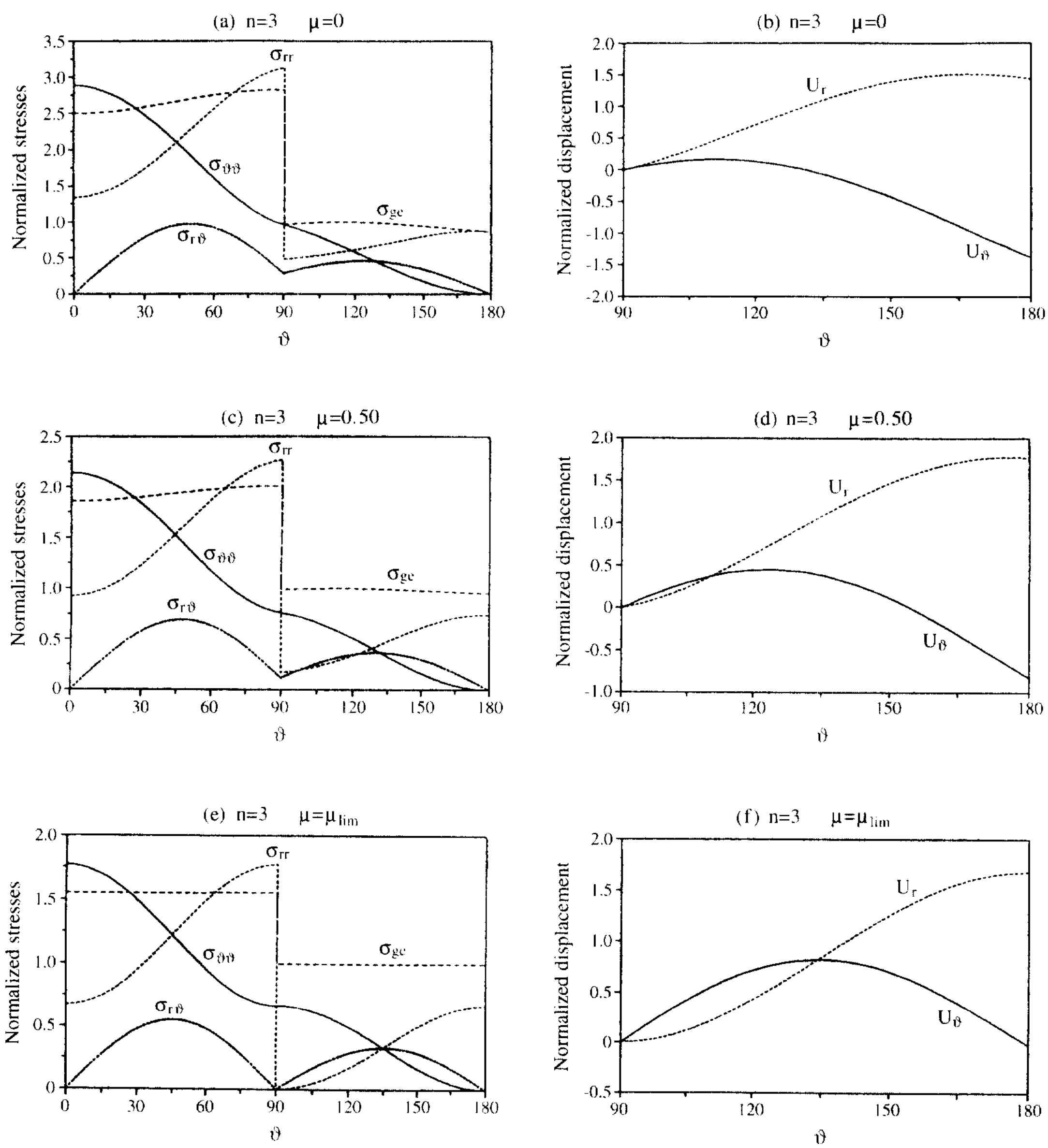

Fig. 9. θ-variation of the stresses $\tilde{\sigma}_{ij}$ and the displacements $\tilde{u}_i$ near the tip of crack II ($n = 3$).

u_θ at $\theta = \pi$ can be greater than zero. Then it means the crack faces may contact with each other, so this case is ruled out for consideration.

Figures 9–11 show the results for the cases with typical values of n and μ. From these figures we can see that a large value of μ results in smaller stresses $\tilde{\sigma}_{ij}$ and only a small jump occurs in the radial stress $\tilde{\sigma}_{rr}$ at the interface. For all the values of n, the radial stress $\tilde{\sigma}_{rr}$ and the shear stress $\tilde{\sigma}_{r\theta}$ near the interface of plastic region are nearly equal to zero.

5. CONCLUSIONS

1. For the two types of cracks, crack I which is lying along the interface and crack II which is perpendicular to the interface between a linear elastic material and a pressure-sensitive dilatant material, we obtain exact asymptotic solutions of plane-stress tip fields which satisfy the continuity of tractions on the interface and the traction-free conditions on the crack faces. The interface strongly affects the stresses within certain region, especially for the radial stress near the interface, where there is a big jump on both sides.

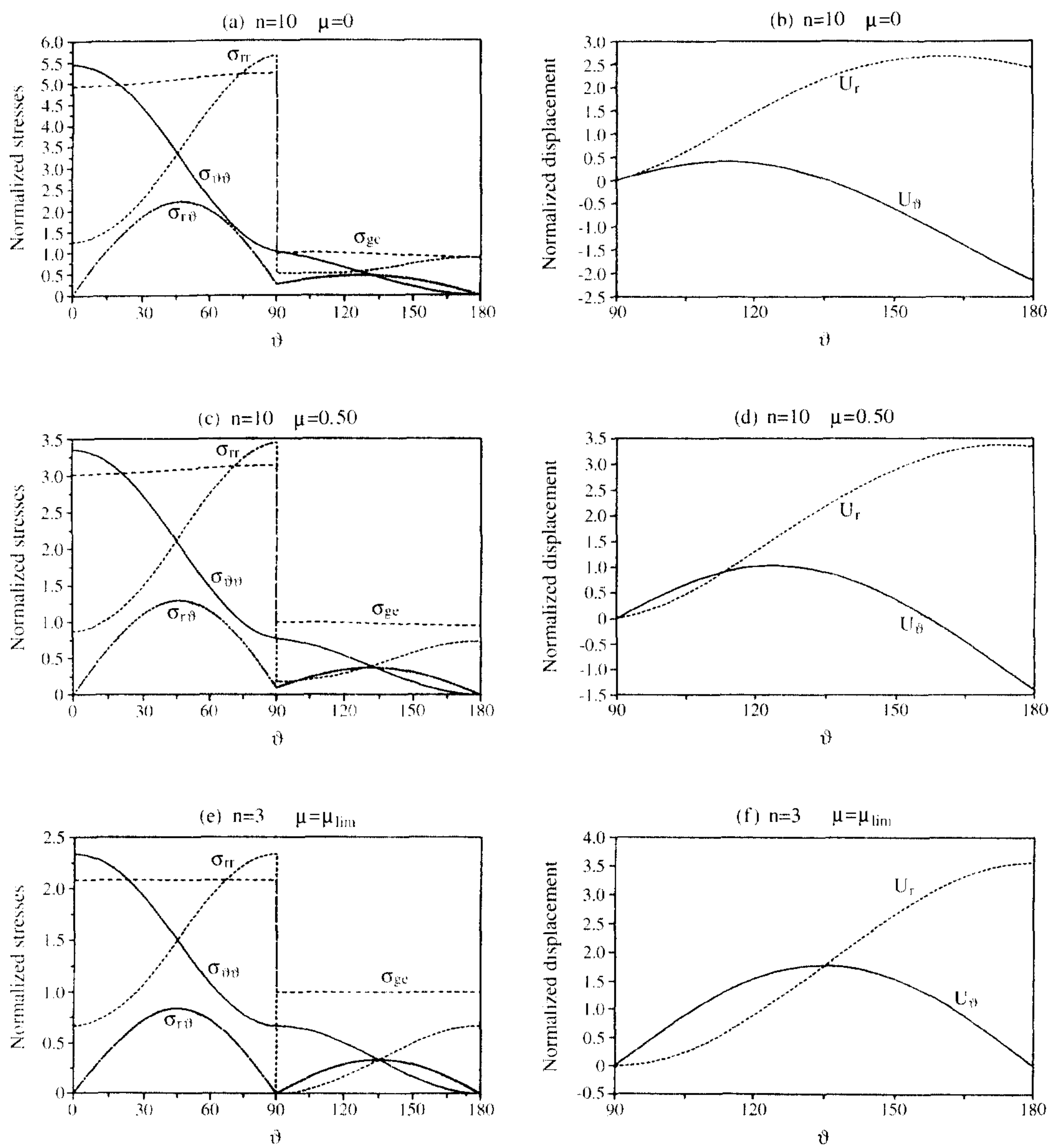

Fig. 10. θ-variation of the stresses $\tilde{\sigma}_{ij}$ and the displacements $\tilde{u}_i$ near the tip of crack II ($n = 10$).

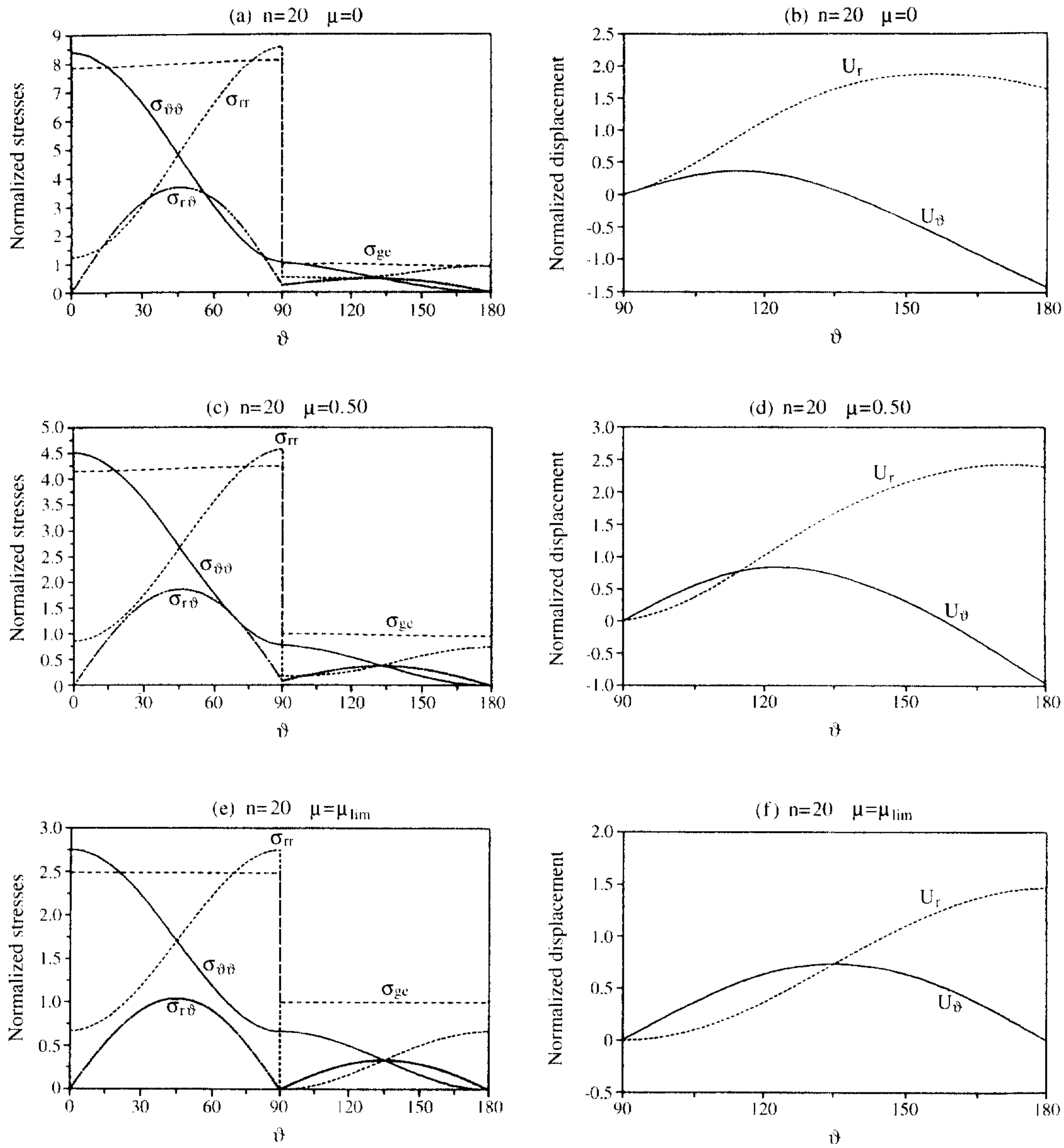

Fig. 11. θ-variation of the stresses $\tilde{\sigma}_{ij}$ and the displacements $\tilde{u}_i$ near the tip of crack II (n = 20).

2. For the crack I, the eigenvalue s is irrelevant to the pressure sensitivity factor μ and is equal to $-1/(n + 1)$ which is also the eigenvalue of the HRR fields in homogenous media without pressure sensitivity. The stress fields near crack tip are generally mixed by mode I and mode II. This characteristic behavior of plane-stress condition is quite different from that of the corresponding plane strain results reported by Yuan[19].
3. For the crack II, s is greater than $-1/(n + 1)$ and increases as μ increases under fixed value of n. s approaches to zero when μ is close to a certain value called $\mu_{\rm lim}$.

Acknowledgements—This work was supported by the National Natural Science Foundation of China, Science Foundation of Chinese Academy of Sciences and Laboratory for Nonlinear Mechanics of Continuous Media, Institute of Mechanics.

REFERENCES

1. Spitzig, W. A. and Richmond, O., Effect of hydrostatic pressure on the deformation behaviour of polythene and polycarbonate in tension and compression. *Polymer Engineering and Science*, 1979, **19,** 1129–1139.
2. Carapellucci, L. M. and Yee, A. F., The biaxial deformation and yield behaviour of bisphenol-a polycarbonate, effect of anisotropy. *Polymer Engineering and Science*, 1986, **26,** 920–930.
3. Sue, H. J. and Yee, A. F., Toughening mechanisms in a multi-phase alloy of nylon 6,6/polyphenylene oxide. *Journal of Material Science*, 1989, **24,** 1447–1457.
4. Chen, I. W. and Morel, P. E. R., Implications of transformation plasticity in ZrO_2-containing ceramics: I shear and dilatation effect. *Journal of the American Ceramic Society*, 1986, **69,** 181–189.
5. Williams, M. L., The stress around a fault or crack in dissimilar media. *Bulletin of the Seismology Society of America*, 1959, **49,** 199–204.
6. Cheepanov, G. P., The stress state in a heterogeneous plate with slits. *Izv. AN SSSR, OTH, Mekhan i Mashin*, 1962, **1,** 131–137.
7. Erdogan, F., Stress distribution in bonded dissimilar materials with cracks. *Journal of Applied Mechanics*, 1965, **32,** 403–410.
8. Sih, G. C. and Rice, J. R., The bending of plates in dissimilar materials with crack. *Journal of Applied Mechanics*, 1963, **30,** 232–236.
9. Rice, J. R. and Sih, G. C., Plane problems of cracks in dissimilar media. *Journal of Applied Mechanics*, 1965, **32,** 400–402.
10. Malyshev, B. M. and Salganik, R. L., The strength of adhesive joints using the theory of cracks. *International Journal of Fracture Mechanics*, 1965, **1,** 114–128.
11. Hutchinson, J. W., Mear, M. and Rice, J. R., Crack paralleling an interface between dissimilar material. *Journal of Applied Mechanics*, 1987, **54,** 828–832.
12. Rice, R. J., Elastic fracture mechanics concepts for interfacial cracks. *Journal of Applied Mechanics*, 1988, **55,** 98–103.
13. Shih, C. F. and Asaro, R. J., Elastic–plastic analysis of cracks on bimaterial interface: part I—small scale yielding. *Journal of Applied Mechanics*, 1988, **55,** 299–316.
14. Zywicz, E. and Park, D. M., Elastic yield zone around an interfacial crack tip. *Journal of Applied Mechanics*, 1989, **56,** 577–584.
15. Shih, C. F. and Asero, R. J., Elastic–plastic and asymptotic fields of interface cracks. *International Journal of Fracture*, 1990, **42,** 101–116.
16. Shih, C. F. and Asaro, R. J., Elastic–plastic analysis of cracks on bimaterial interface: part II—structure of small scale yielding. *Journal of Applied Mechanics*, 1989, **56,** 763–779.
17. Parks, D. M. and Zywick, E., Elastic/perfectly-plastic small scale yielding at bimaterial interfaces. In *Advances in Fracture Research*, Vol. 4, ed. Salama *et al.*, 1989, pp. 3081–3088.
18. Wang, T. C., Elastic–plastic asymptotic fields for cracks on bimaterial interfaces. *Engineering Fracture Mechanics*, 1990, **37,** 527–538.
19. Yuan, H., Elastoplastic crack analysis for pressure-sensitive dilatant material—part II: interface cracks. *International Journal of Fracture*, 1994, **69,** 167–187.
20. Drucker, D. C. and Prager, W., Soil mechanics and plastic analysis or limit design. *Quarterly Journal of Applied Mathematics*, 1952, **10,** 157–165.
21. Li, F. Z. and Pan, J., Plane-strain crack-tip fields for pressure-sensitive dilatant materials. *Journal of Applied Mechanics*, 1990, **57,** 40–47.
22. Shih, C. F., Small scale yielding analysis of mixed mode plane strain crack problem. *Fracture Analysis, ASTM STP*, 1974, **560,** 187–210.

(*Received* 6 *November* 1996, *in final form* 27 *July* 1997, *accepted* 27 *July* 1997)